引用格式：XIA Tian, CHEN Weijun, SUN Boxuan, et al. Defect Solitons in PT-symmetric Optical Lattices with Fractional Diffraction[J]. Acta Photonica Sinica, 2026, 55(2):0219003
夏天,陈卫军,孙博轩,等.分数衍射下PT对称光学格子中的缺陷孤子[J].光子学报,2026,55(2):0219003

分数衍射下PT对称光学格子中的缺陷孤子

夏天,陈卫军,孙博轩,王靖雨,吴楚瑶,夏浩然,赵鹏,王连锴,宋德
(长春理工大学 物理学院,长春 130022)

摘　要:研究了分数阶克尔非线性薛定谔方程中PT对称光学格子中缺陷孤子的存在性、稳定性和动力学特性。结果表明:光学格子的带隙范围随着Lévy指数的减小而变宽,随着晶格缺陷强度从负到正增加,半无穷带隙范围逐渐变窄,其他带隙范围则逐渐变窄。在分数衍射下,随着Lévy指数的增加,对于所有缺陷晶格,半无穷带隙和第一带隙内缺陷孤子的功率逐渐变大,孤子的稳定性越来越好。负缺陷和零缺陷情况下,缺陷孤子仅在半无穷带隙存在稳定区间,在第一带隙全不稳定,正缺陷情况下,缺陷孤子在半无穷带隙和第一带隙内均存在稳定区间。此外,在半无穷带隙内,随Lévy指数的减小,缺陷孤子包络的峰值增加,宽度变窄,随着传播常数的增加,缺陷孤子包络的峰值迅速减小;在第一带隙内,正缺陷情况下孤子包络的峰值随Lévy指数的减小而变小,随传播常数绝对值的增加而变大。

关键词:非线性光学;宇称时间对称;缺陷孤子;分数衍射;克尔效应
中图分类号:O437　　**文献标识码**:A　　**doi**:10.3788/gzxb20265502.0219003

0　引言

分数效应在物理学多个领域催生了许多新奇现象,例如分数量子霍尔效应、量子分数谐振子、分数约瑟夫森效应以及分数塔尔博特效应等[1-4]。2000年,LASKIN N[5-7]为了描述费曼路径积分中的布朗轨迹被Lévy飞行取代时的分数量子力学,理论上提出了分数阶薛定谔方程,这一开创性工作极大地推动了相关领域的深入研究。2015年,LONGHI S[8]在非球形光学腔中首次实验实现了空间分数衍射效应,分数阶薛定谔方程被拓展至光学领域。此后,研究人员利用分数效应调控光场传输,产生了一系列新颖的光学现象,如啁啾高斯光束的调制动力学[9-10]、无衍射光束的产生[11]、光束传输调控[12]、光学布洛赫振荡与齐纳隧穿[13]、艾里光束调控[14-16]及分数涡旋光束[17]等。2023年,研究人员利用可编程全息成像技术和单镜头测量技术实现分数色散,在时间域上实验实现了分数阶薛定谔方程,并观察到时间孤子、脉冲分裂等分数色散系统中的新颖现象[18]。

宇称时间(Parity-Time, PT)对称性的概念源自量子力学,满足宇称变换和时间反演变换对称的非厄米哈密顿量具有全实谱[19],PT对称性将增益与损耗整合进同一系统,使其在对称相呈现实数能谱以维持稳定动力学,这一特性为在非厄米体系中操控波的传输与相变提供了核心原理,实验中可以通过引入具有增益损耗的复数型折射率分布在光学结构上实现PT对称光学系统[20],光场在该系统中传输时可表现出独特特性,如单向不可见性[21]、光能量振荡[22]、非厄米趋肤效应[23]、非互易光传输[24]等。近20年来,大量文献工作报道了正常衍射下PT对称的不同非线性光学格子中的孤子,包括一维和二维空间孤子[22-26]、带隙孤子[27]、多极孤子[28]、缺陷孤子[29]、矢量孤子[30]、灰孤子[31]等。

引入分数衍射效应后,PT对称势场下的孤子表现出了丰富的特性,例如,在自聚焦克尔非线性PT对称

基金项目:吉林省自然科学基金(YDZJ202301ZYTS377),国家自然科学基金(U2141239,12274041),吉林省光电子探测与多维信息处理工程研究中心自主创新能力建设项目(2021C032)
第一作者:夏天,xtian0606@163.com
通讯作者:陈卫军,chenweijun@cust.edu.cn;宋德,songde614@163.com
收稿日期:2025-09-10;**录用日期**:2025-10-12

光学格子中，孤子的稳定区域随着PT对称势虚部的增加而迅速收缩，直至消失[32]，并且矢量孤子的存在性、稳定性及其包络结构也会随Lévy指数显著变化[33]。在自散焦克尔非线性PT对称光学格子中，发现同相位三极孤子和四极带隙孤子可存在于第一带隙内，且Lévy指数不仅影响孤子的稳定区域，还影响多极孤子的宽度[34]。同时，调节Lévy指数可以控制基本孤子的形态变化[35]，也可观察到二维孤子自发对称破缺及鬼态现象[36]。在散焦饱和非线性PT对称光学格子中，二维基本孤子和同相位偶极孤子的稳定区域随着Lévy指数的减小而变小，并且饱和参数对孤子的存在性和稳定性也有显著影响[37]，再者，PT对称势调制强度和Lévy指数的增大可使多极孤子的存在域逐渐扩展[38]。在聚焦饱和非线性部分PT对称光学格子中，增强分数衍射效应使得二维光孤子的稳定性变弱，引起小功率孤子发生自发对称破缺[39]。在竞争型PT对称光学格子中可以存在偶极孤子和三极孤子，并且Lévy指数越大，这两类孤子的稳定区域越大[40-41]。在PT对称分数阶耦合器中，孤子会因分数阶色散与立方非线性作用发生自发对称性破缺分岔，并且PT对称孤子的失稳会引发对称性破缺并产生鬼态[42]。另一方面，如果在光学格子的格点处引入缺陷，当线性缺陷模的传播常数位于非线性光学格子的带隙内时，可以形成在缺陷区域自陷传输的缺陷孤子，迄今为止，关于正常衍射和分数衍射机制下缺陷孤子的存在性和稳定性研究已有大量文献报道[29, 43-53]。然而，在分数效应与PT对称势共同作用下光学格子中的缺陷孤子的存在性和稳定性尚未见详细报道。

本文主要研究分数衍射下PT对称光学格子中的缺陷孤子的存在性、稳定性及传输动力学特性，探究分数效应和缺陷类型对能带结构的影响，分析缺陷孤子的存在域，阐释缺陷孤子的线性稳定性，讨论系统参数对缺陷孤子特征的影响。

1 理论模型

考虑分数效应，在具有PT对称势的克尔非线性光学格子中，光波传输满足的1+1维无量纲演化方程为[29-30,32]

$$\mathrm{i}\frac{\partial q}{\partial z}-\left(-\frac{\partial^2}{\partial x^2}\right)^{\alpha/2}q+R(x)q+|q|^2q=0 \tag{1}$$

式中，x和z分别是被光场初始宽度和衍射长度归一化后的横坐标和纵坐标，α是描述分数衍射的Lévy指数（$1<\alpha\leqslant 2$），PT对称势函数$R(x)=p[V(x)+\mathrm{i}W(x)]$，$p$是PT对称势的深度，$V(x)=\cos^2(x)[1+\varepsilon\exp(-x^8/128)]$表示PT对称势的实部，$W(x)=W_0\sin 2x$表示PT对称势的虚部，$f(x)=\exp(-x^8/128)$是描述缺陷形式的局部函数，$\varepsilon$是缺陷强度系数，$\varepsilon<0$表示负缺陷类型，$\varepsilon>0$表示正缺陷类型。本文仅考虑对称势的虚部调制深度$W_0$低于相变点（$W_0=0.5$）情况下分数效应对缺陷孤子的影响，因此，参数取值为$p=3$，$W_0=0.1$。

为寻求式（1）的孤子解，假设孤子解形式为$q(x,z)=u(x)\exp(-\mathrm{i}bz)$，将该表达式代入式（1）并简化可得

$$\left(-\frac{\partial^2}{\partial x^2}\right)^{\alpha/2}u+p\left[V(x)+\mathrm{i}W(x)\right]u+|u|^2u+bu=0 \tag{2}$$

式中，$u(x)$是孤子的振幅函数，b是传播常数。可采用改进的平方算子法[54]对式（2）进行数值求解，得到孤子的解。

为了研究PT对称光学格子的带隙结构，不考虑非线性时，根据布洛赫定理，式（1）的解可以写为

$$q(x,z)=u_k(x)\exp(\mathrm{i}kz-\mathrm{i}bz) \tag{3}$$

式中，$u_k(x)$是布洛赫模。运用平面波展开法，式（1）得到的本征方程为

$$\sum_n A_{m-n}B_n-|k+K_m|^\alpha A_m=-bA_m \tag{4}$$

式中，周期函数$u_k(x)$满足$u_k(x)=u_k(x+T)$，T是周期，$K_m=2m\pi/T$，$u_k(x)=\sum_m A_m\exp(\mathrm{i}K_mx)$，$R(x)=\sum_n B_n\exp(\mathrm{i}K_nx)$，$A_m=\int_0^T u_k(x)\exp(-\mathrm{i}K_mx)\mathrm{d}x\Big/T$，$B_n=\int_0^T R(x)\exp(-\mathrm{i}K_nx)\mathrm{d}x\Big/T$。

为了分析缺陷孤子的线性稳定性，设式（1）的扰动解为

$$q(x,z)=\left\{u(x)+\left[v(x)-w(x)\right]\mathrm{e}^{\delta z}+\left[v(x)+w(x)\right]^{*}\mathrm{e}^{\delta^{*}z}\right\}\mathrm{e}^{-\mathrm{i}bz} \tag{5}$$

式中，$v(x)$和$w(x)$是无穷小扰动，$v(x),w(x)\ll 1$，上标*表示复共轭，δ表示扰动增长率。将式(5)代入式(1)，可以化为以下特征值问题

$$-\mathrm{i}\begin{bmatrix}-\mathrm{i}pW-\mathrm{iIm}(u^{2}) & F+pV-\mathrm{Re}(u^{2})\\ F+pV+\mathrm{Re}(u^{2}) & -\mathrm{i}pW+\mathrm{iIm}(u^{2})\end{bmatrix}=\delta\begin{bmatrix}v\\ w\end{bmatrix} \tag{6}$$

式中，$F=-\left(-\dfrac{\partial^{2}}{\partial x^{2}}\right)^{\alpha/2}+2|u|^{2}+b$。可以利用傅里叶配置法[54]对特征值$\delta$进行求解。若其实部$\mathrm{Re}(\delta)=0$，则缺陷孤子是线性稳定的，否则，缺陷孤子是不稳定的。

2 研究结果及讨论

图1展示了在不同缺陷条件下PT对称光学晶格的强度分布、能带结构及带隙范围。其中图1(a)～(c)分别展示了负缺陷($\varepsilon=-0.5$)、零缺陷($\varepsilon=0$)及正缺陷($\varepsilon=0.5$)时具有PT对称势的晶格强度曲线，可以看出，负缺陷表现为晶格势场在缺陷位置呈现局部凹陷，零缺陷对应均匀势场分布的晶格结构，正缺陷表现为

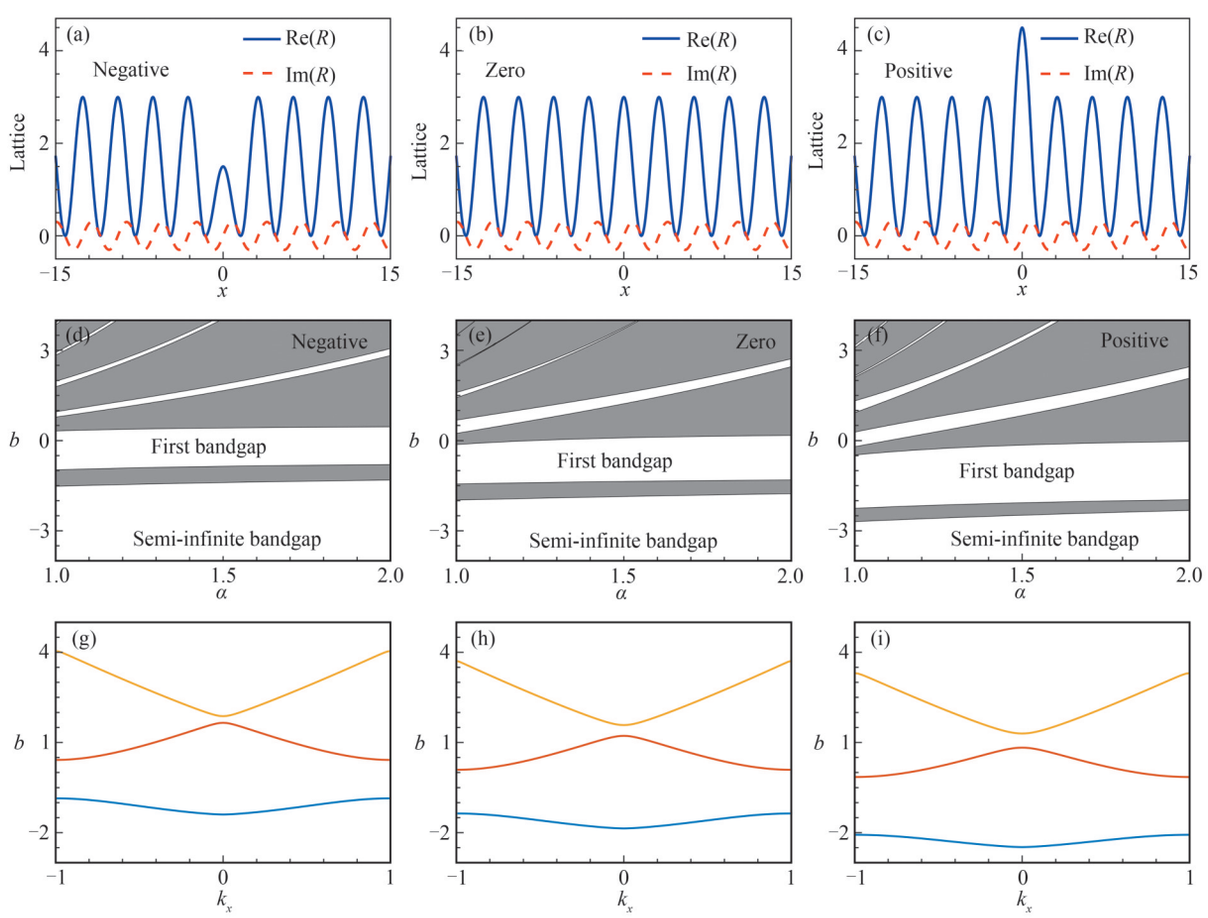


图1 不同缺陷类型的晶格强度曲线、能带结构和带隙范围。(a)负缺陷($\varepsilon=-0.5$)晶格强度曲线；(b)零缺陷($\varepsilon=0$)晶格强度曲线；(c)正缺陷($\varepsilon=0.5$)晶格强度曲线；(d)负缺陷($\varepsilon=-0.5$)能带结构；(e)零缺陷($\varepsilon=0$)能带结构；(f)正缺陷($\varepsilon=0.5$)能带结构；(g)$\alpha=1.5$时负缺陷($\varepsilon=-0.5$)带隙范围；(h)$\alpha=1.5$时零缺陷($\varepsilon=0$)带隙范围；(i)$\alpha=1.5$时正缺陷($\varepsilon=0.5$)带隙范围

Fig. 1 Lattice profiles, band structures, and band gap ranges for different types of defects. (a) Lattice profile with a negative defect ($\varepsilon=-0.5$); (b) Lattice profile with zero defect ($\varepsilon=0$); (c) Lattice profile with a positive defect ($\varepsilon=0.5$); (d) Band structure with a negative defect ($\varepsilon=-0.5$); (e) Band structure with zero defect ($\varepsilon=0$); (f) Band structure with a positive defect ($\varepsilon=0.5$); (g) Bandgap range with a negative defect ($\varepsilon=-0.5$) at $\alpha=1.5$; (h) Bandgap range with zero defect ($\varepsilon=0$) at $\alpha=1.5$; (i) Bandgap range with a positive defect ($\varepsilon=0.5$) at $\alpha=1.5$

缺陷位置的势场局部凸起。图1(d)～(f)分别给出了上述三种缺陷对应的能带结构，可以发现，随着缺陷强度从负到正增加，半无穷带隙范围变窄，第一和第二带隙范围变宽。图1(g)～(i)给出了$\alpha=1.5$时对应上述三种缺陷类型的带隙范围，此时，计算得到不同缺陷类型对应的共同半无穷带隙和第一带隙范围分别为$b>-1.977\,2$和$-1.312\,7<b<-0.132\,0$。值得注意的是，分数衍射下不同带隙的范围也随着α的变化而变化，不同缺陷情况下半无穷带隙范围随着α的减小而逐渐减小。可见，改变Lévy指数α和缺陷强度ε可以调控光学格子的带隙范围。

接下来，考虑在分数衍射效应缺陷类型分别为负缺陷、零缺陷及正缺陷情况下缺陷孤子的性质。首先，负缺陷时($\varepsilon=-0.5$)，图2(a)给出了α取不同值时缺陷孤子的功率P随传播常数b变化的曲线，其中缺陷孤子的功率定义为$P=\int_{-\infty}^{+\infty}|u|^2\,\mathrm{d}x$。可以看出，在半无穷带隙内，缺陷孤子的功率随着$\alpha$单调递增，在高功率区随着传播常数的增加而减小，值得注意的是，在低功率区(即在半无穷带隙边界范围附近)，缺陷孤子的功率出现先略微增大后减小的现象。在第一带隙内，缺陷孤子的功率仍然随着传播常数的增加而减小，但在中功率区出现先略微增大后减小的现象。通过图2(b)中的增长率与传播常数关系曲线可以看出，随着α值的减小，$\mathrm{Re}(\delta)\neq0$的范围越来越大，半无穷带隙内缺陷孤子的稳定性变差，即稳定孤子的存在范围越来越窄。在第一带隙内缺陷孤子全不稳定。为了验证缺陷孤子的传输稳定性，图2(c)～(f)分别计算了不同带隙中的孤子包络，分别对应于图2(a)和(b)中的$A(\alpha=1.2,b=-3.1)$、$B(\alpha=1.5,b=-4)$、$C(\alpha=1.8,b=-2.5)$、

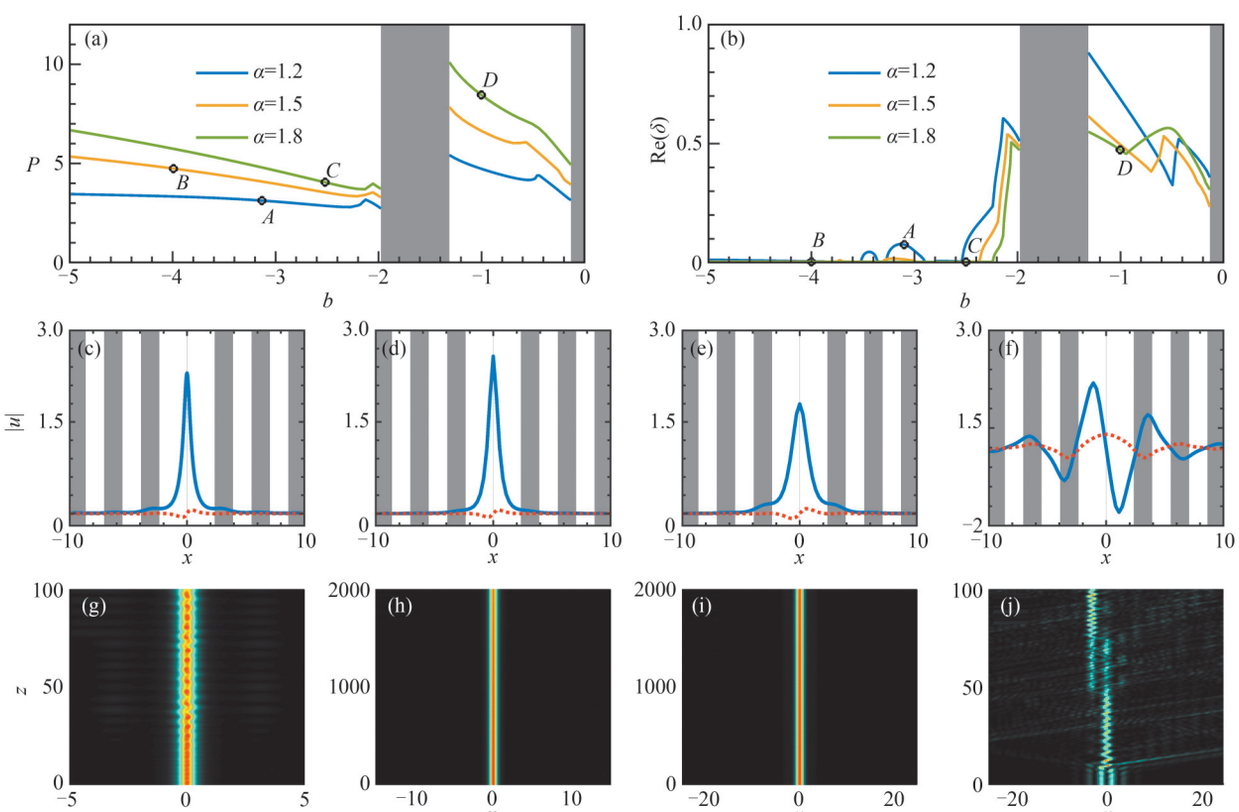


图2 负缺陷晶格($\varepsilon=-0.5$)中孤子的功率、稳定性、包络及其演化图。(a) 不同Lévy指数下半无穷带隙和第一带隙中缺陷孤子的功率P与传播常数b的关系；(b) 不同Lévy指数下扰动增长率$\mathrm{Re}(\delta)$与传播常数b的关系；(c)～(f) 图(a)或(b)中$A(b=-3.1,\ \alpha=1.2)$、$B(b=-4,\ \alpha=1.5)$、$C(b=-2.5,\ \alpha=1.8)$、$D(b=-1,\ \alpha=1.8)$点处分别对应的缺陷孤子包络；(g)～(j) 图(c)～(f)中孤子包络在施加10%高斯随机噪声后的演化图

Fig. 2 Power, stability, envelope and evolution diagrams of solitons in negative defect lattices ($\varepsilon=-0.5$). (a) Power P versus propagation constant b for defect solitons in the semi-infinite gap and the first gap under different Lévy indices; (b) Perturbation growth rate $\mathrm{Re}(\delta)$ versus propagation constant b under different Lévy indices; (c)～(f) Defect soliton envelopes corresponding to points $A(b=-3.1,\ \alpha=1.2)$、$B(b=-4,\ \alpha=1.5)$、$C(b=-2.5,\ \alpha=1.8)$、$D(b=-1,\ \alpha=1.8)$ in Fig. (a) or (b), respectively; (g)～(j) Evolution of the soliton envelopes in (c)～(f) under 10% Gaussian random noise perturbation

$D(\alpha=1.8, b=-1)$点，并以这些孤子作为初始条件，对其添加10%的随机高斯噪声扰动，采用分步傅里叶法对孤子的传输进行演化，结果分别如图2(g)～(j)所示。可以看出，A点和D点对应的缺陷孤子在传输较短距离时出现不稳定情况，而B点和C点对应的缺陷孤子在传输较长距离后仍可以保持其波形不变，这与图2(b)所示的稳定性一致。

对于零缺陷($\varepsilon=0$)情况，α取不同值时缺陷孤子的功率随传播常数变化曲线如图3(a)所示，可以看出，在半无穷带隙和第一带隙内，缺陷孤子的功率随传播常数的增加逐渐减小，随α的增加逐渐增大。从图3(b)可以看出，在半无穷带隙内，当α较大($\alpha=1.5$或1.8)时，缺陷孤子是稳定的，当较小($\alpha=1.2$)时，在不同带隙区间出现缺陷孤子不稳定的范围，即缺陷孤子的稳定性变差，在第一带隙内，$\mathrm{Re}(\delta)\neq0$，表明缺陷孤子是全不稳定的。同样，为了验证这些稳定性，分别计算了不同参数条件下的孤子解，其包络如图3(c)～(f)所示，分别对应于图3(a)和(b)中的$A(\alpha=1.2, b=-6.5)$、$B(\alpha=1.5, b=-4)$、$C(\alpha=1.8, b=-3)$、$D(\alpha=1.8, b=-0.5)$点，在10%的随机高斯噪声扰动下，这些孤子的传输过程分别如图3(g)-(j)所示，与图2相似，A点和D点对应的缺陷孤子在传输较短距离时出现不稳定情况，而B点和C点对应的缺陷孤子在传输较长距离后仍可以保持其波形不变。值得注意的是，图3(b)中B点和C点之间存在微小凸起，其缺陷孤子与A点缺陷孤子的传输类似，出现不稳定情况，进一步验证了图3(b)所示的稳定性。

在正缺陷($\varepsilon=0.5$)情况下，图4给出了缺陷孤子的功率变化、扰动增长率、孤子包络及演化特性。从图4(a)可以看出，在半无穷带隙和第一带隙内，缺陷孤子的功率随传播常数单调递减，随α单调递增。值得注意的

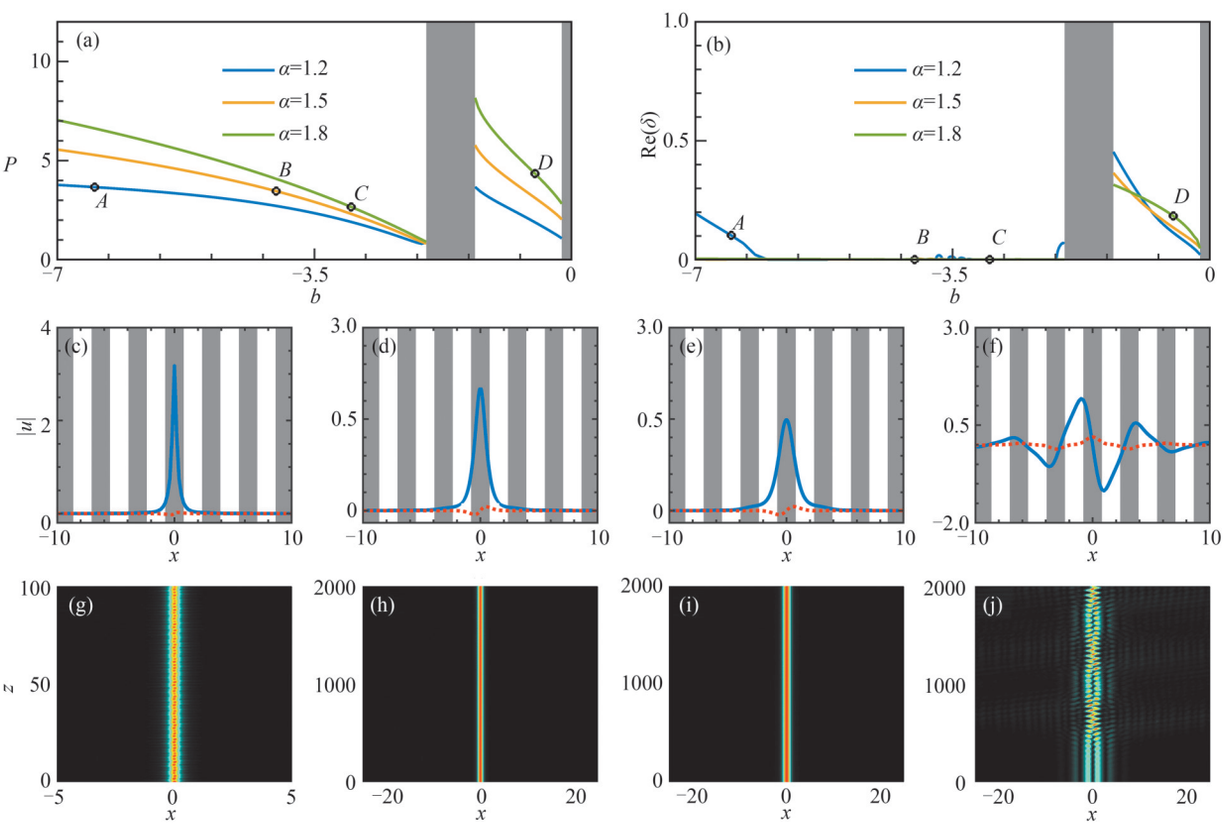


图3 零缺陷晶格($\varepsilon=0$)中孤子的功率、稳定性、包络及其演化图。(a) 不同Lévy指数下半无穷带隙和第一带隙中缺陷孤子的功率P与传播常数b的关系；(b) 不同Lévy指数下扰动增长率$\mathrm{Re}(\delta)$与传播常数b的关系；(c)～(f) 图(a)或(b)中$A(b=-6.5, \alpha=1.2)$、$B(b=-4, \alpha=1.5)$、$C(b=-3, \alpha=1.8)$、$D(b=-0.5, \alpha=1.8)$点处分别对应的缺陷孤子包络；(g)～(j) 图(c)～(f)中孤子包络在施加10%高斯随机噪声后的演化图

Fig. 3 Power, stability, envelope and evolution diagrams of solitons in zero defect lattices ($\varepsilon=0$). (a) Power P versus propagation constant b for defect solitons in the semi-infinite gap and the first gap under different Lévy indices; (b) Perturbation growth rate $\mathrm{Re}(\delta)$ versus propagation constant b under different Lévy indices; (c)～(f) Defect soliton envelopes corresponding to points $A(b=-6.5, \alpha=1.2)$、$B(b=-4, \alpha=1.5)$、$C(b=-3, \alpha=1.8)$、$D(b=-0.5, \alpha=1.8)$ in Fig. (a) or (b), respectively; (g)～(j) Evolution of the soliton envelopes in (c)～(f) under 10% Gaussian random noise perturbation

是，在半无穷带隙内，存在使缺陷孤子的功率减小到零的传播常数截止点，且α越大，该截止点对应的传播常数值越大，在第一带隙内，仅在α较小时存在截止点。图4(b)给出了正缺陷情况下扰动增长率随传播常数的变化曲线，可以看出，在半无穷带隙内，随着α的减小，$\mathrm{Re}(\delta)\neq 0$的范围逐渐变大，即缺陷孤子的稳定性变差，在第一带隙内，存在部分区间满足$\mathrm{Re}(\delta)=0$，即存在稳定的缺陷孤子。为了验证这些稳定性，图4(c)～(f)分别给出了几种不同参数条件下的缺陷孤子包络，分别对应于图4(a)和(b)中的$A(\alpha=1.2, b=-6.5)$、$B(\alpha=1.5, b=-4)$、$C(\alpha=1.8, b=-3)$、$D(\alpha=1.5, b=-0.3)$点，在10%的随机高斯噪声扰动下，这些孤子的演化分别如图4(g)～(j)所示，可以看出，A点对应的缺陷孤子在传输时是不稳定的，而B、C及D点对应的缺陷孤子在传输较长距离后仍可以保持其稳定性，与图4(b)所示的稳定性吻合。

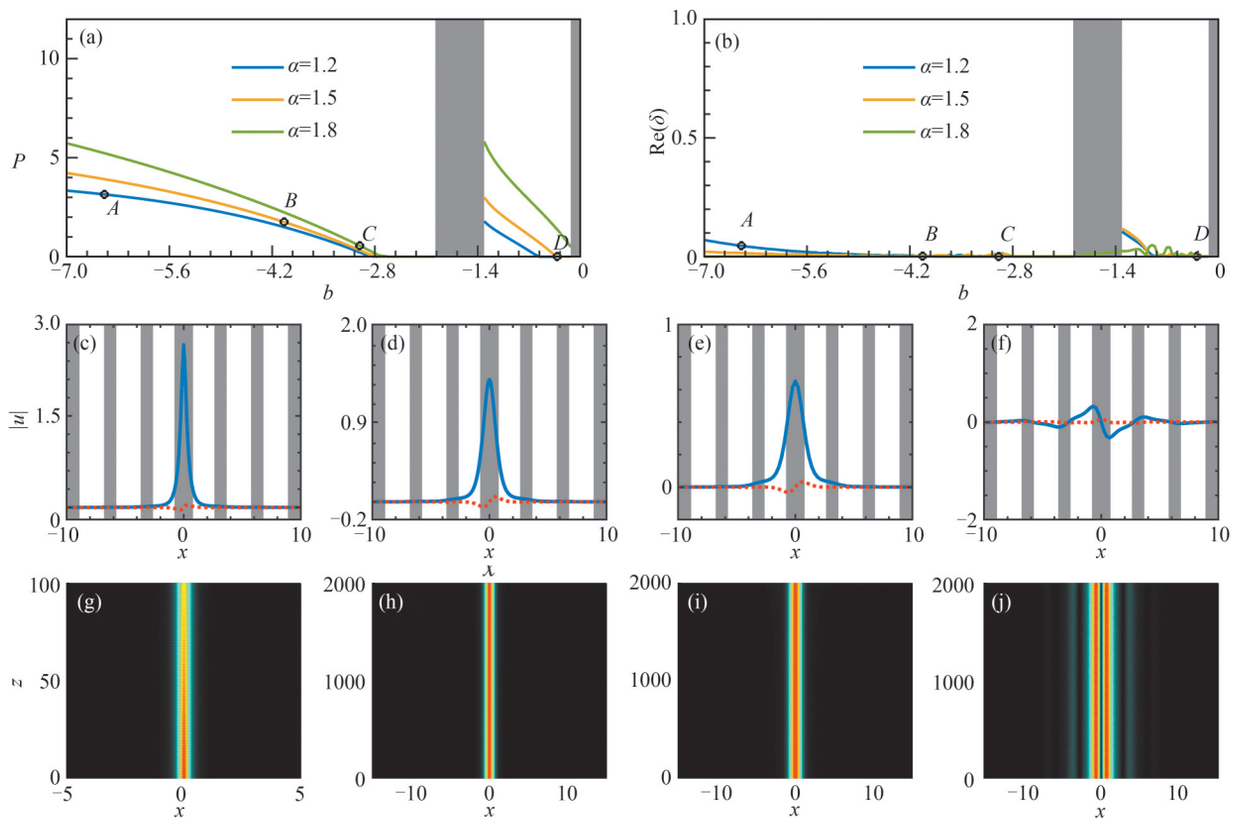


图4 正缺陷晶格($\varepsilon=0.5$)中孤子的功率、稳定性、包络及其演化图。(a) 不同Lévy指数下半无穷带隙和第一带隙中缺陷孤子的功率P与传播常数b的关系；(b) 不同Lévy指数下扰动增长率$\mathrm{Re}(\delta)$与传播常数b的关系；(c)～(f) 图(a)或(b)中$A(b=-6.5, \alpha=1.2)$、$B(b=-4, \alpha=1.5)$、$C(b=-3, \alpha=1.8)$、$D(b=-0.3, \alpha=1.5)$点处分别对应的缺陷孤子包络；(g)～(j) 图(c)～(f)中孤子包络在施加10%高斯随机噪声后的演化图

Fig. 4 Power, stability, envelope and evolution diagrams of solitons in positive defect lattices ($\varepsilon=0.5$). (a) Power P versus propagation constant b for defect solitons in the semi-infinite gap and the first gap under different Lévy indices; (b) Perturbation growth rate $\mathrm{Re}(\delta)$ versus propagation constant b under different Lévy indices; (c)～(f) Defect soliton envelopes corresponding to points $A(b=-6.5, \alpha=1.2)$、$B(b=-4, \alpha=1.5)$、$C(b=-3, \alpha=1.8)$、$D(b=-0.3, \alpha=1.5)$ in Fig. (a) or (b), respectively; (g)～(j) Evolution of the soliton envelopes in (c)～(f) under 10% Gaussian random noise perturbation

为了详细分析系统参数对缺陷孤子特征的影响，图5详细给出了分数衍射下系统参数对稳定的缺陷孤子包络的影响。图5(a)给出了ε取不同值时缺陷孤子的功率P随传播常数变化b的曲线，相同条件下缺陷孤子的功率随缺陷强度从负到正增加而减小。图5(b)给出了不同缺陷强度下扰动增长率随传播常数的变化曲线，缺陷孤子的稳定性随缺陷强度从负到正增加而增加。图5(c)～(e)分别是半无穷带隙内负、零、正三种晶格缺陷下α取不同值时的缺陷孤子包络，可以看出，缺陷孤子包络的宽度随α的减小缓慢变窄，峰值随α的减小缓慢变大，且孤子包络的峰值随着缺陷强度从负到正增加而减小，图5(f)给出的是正缺陷条件下第一带隙内缺陷孤子的包络，缺陷孤子包络的宽度变化规律与半无穷带隙一致，但峰值随α的减小而变小。

图5(g)～(i)分别是半无穷带隙内负、零、正三种晶格缺陷下传播常数取不同值时的缺陷孤子包络，显然，随着传播常数的增加，缺陷孤子包络的峰值迅速减小。在第一带隙内，正缺陷条件下的孤子包络如图5(j)所示，不同的是，此时孤子包络峰值随着传播常数的增加而减小，从包络曲线亦可看出，孤子功率随传播常数绝对值的增加而变大。

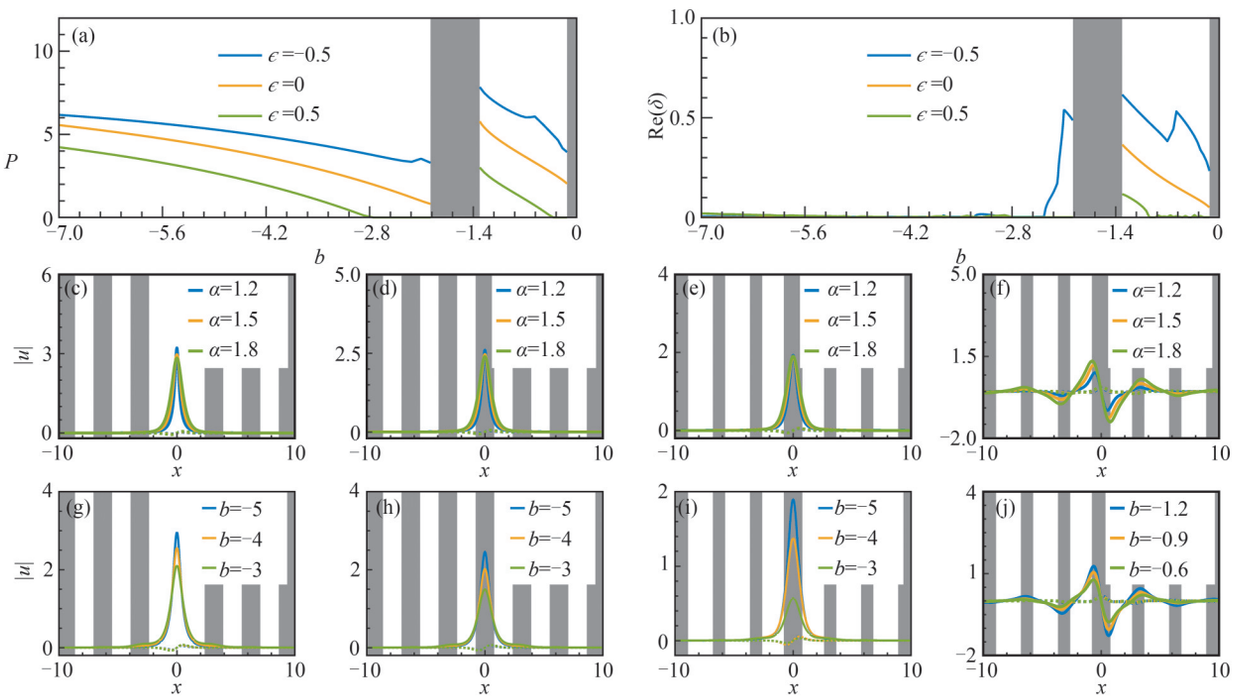


图5 系统参数对缺陷孤子特征的影响。(a)半无穷带隙和第一带隙中选定的$\alpha=1.5$时，缺陷孤子的功率P与传播常数b的关系；(b)扰动增长率Re(δ)与传播常数b的关系；(c)-(e)选定的α，$b=-5$和缺陷强度$\varepsilon=-0.5$，0和0.5时半无穷带隙缺陷孤子轮廓；(f)正缺陷$\varepsilon=0.5$选定的α和$b=-1$时第一带隙缺陷孤子轮廓；(g)-(i)选定的$\alpha=1.5$，b时缺陷强度$\varepsilon=-0.5$，0和0.5时半无穷带隙缺陷孤子轮廓；(j)正缺陷$\varepsilon=0.5$选定的$\alpha=1.5$和b时第一带隙缺陷孤子轮廓

Fig. 5 The influence of system parameters on the characteristics of defect solitons. (a) Power P versus propagation constant b for defect solitons in the semi-infinite gap and the first gap, selected at $\alpha=1.5$; (b) Perturbation growth rate Re(δ) versus propagation constant b; (c)～(e) Envelopes of semi-infinite gap defect solitons for selected α, $b=-5$, and defect strengths $\varepsilon=-0.5$, 0, and 0.5; (f) Envelope of a first-gap defect soliton for a positive defect $\varepsilon=0.5$, with selected α and $b=-1$; (g)～(i) Envelopes of semi-infinite gap defect solitons for selected $\alpha=1.5$, b, and defect strengths $\varepsilon=-0.5$, 0, and 0.5; (j) Envelope of a first-gap defect soliton for a positive defect $\varepsilon=0.5$, with selected $\alpha=1.5$ and b

3 结论

本文研究了分数衍射下具有PT对称势光学格子中的缺陷孤子的存在性、稳定性和传输动力学特性。在分数衍射下，不同缺陷类型的光学格子的带隙范围随着缺陷强度不断变化，半无穷带隙范围随着缺陷强度的不断增加而压缩，其余带隙则与之相反；同时，Lévy指数α的减小会使光学格子的半无穷带隙范围略微缩小。负缺陷情况下，半无穷带隙和第一带隙内的孤子功率随传播常数的增大而逐渐减小，仅在半无穷带隙的低功率区和第一带隙的中功率区出现先增加后减小的情况，孤子在半无穷带隙内的稳定性随α的减小而变差，即稳定范围逐渐缩短，孤子在第一带隙内不稳定。零缺陷情况下，半无穷带隙和第一带隙内的孤子功率随传播常数单调递减，α对孤子的稳定性影响与负缺陷情况类似。正缺陷情况下，半无穷带隙和第一带隙内的孤子功率随传播常数的增大而逐渐减小，但存在功率为零的截止点，且α越小，截止点处的传播常数值越小，同样，α的减小会使得孤子在半无穷带隙的稳定区间变小，但孤子在第一带隙存在稳定区间。此外，三种缺陷类型下，缺陷孤子包络的宽度随α的减小缓慢变窄，功率随α的减小而变小，且孤子包络的峰值随着缺陷强度从负到正增加而减小，在半无穷带隙中峰值随α的减小缓慢变大，而第一带隙则与之相反。总之，缺陷孤子的包络、功率及其稳定性在很大程度上取决于缺陷强度、莱维指数和传播常数。

参考文献

[1] LAUGHLIN R B. Anomalous quantum Hall effect: an incompressible quantum fluid with fractionally charged excitations [J]. Physical Review Letters, 1983, 50(18): 1395-1398.

[2] OLIVAR-ROMERO F, ROSAS-ORTIZ O. Factorization of the quantum fractional oscillator [J]. Journal of Physics: Conference Series, 2016, 698(1): 012025-012025.

[3] ROKHINSON L P, Liu Xinyu, FURDYNA K J. The fractional a. c. Josephson effect in a semiconductor-superconductor nanowire as a signature of Majorana particles[J]. Nature Physics, 2012, 8(11): 795-799.

[4] WEN Jianming, ZHANG Yong, XIAO Min. The Talbot effect: recent advances in classical optics, nonlinear optics, and quantum optics[J]. Advances in Optics and Photonics, 2013, 5(1): 83-130.

[5] LASKIN N. Fractional quantum mechanics and Lévy path integrals[J]. Physics Letters A, 2000, 268(4-6): 298-305.

[6] LASKIN N. Fractional quantum mechanics[J]. Physical Review E, 2000, 62(3): 3135-3145.

[7] LASKIN N. Fractional Schrödinger equation[J]. Physical Review E, 2002, 66(5): 056108.

[8] LONGHI S. Fractional Schrödinger equation in optics[J]. Optics Letters, 2015, 40(6): 1117-1120.

[9] ZHANG Yiqi, LIU Xing, BELIĆ M R, et al. Propagation dynamics of a light beam in a fractional Schrödinger equation[J]. Physical Review Letters, 2015, 115(18): 180403.

[10] ZANG Feng, WANG Yan, LI Lu. Dynamics of Gaussian beam modeled by fractional Schrödinger equation with a variable coefficient[J]. Optics Express, 2018, 26(18): 23740-23750.

[11] ZHANG Yiqi, ZHONG Hua, BELIĆ M R, et al. Diffraction-free beams in fractional Schrödinger equation[J]. Scientific Reports, 2016, 6(1): 23645.

[12] HUANG Changming, DONG Liangwei. Beam propagation management in a fractional Schrödinger equation[J]. Scientific Reports, 2017, 7(1): 5442.

[13] ZHANG Yiqi, WANG Rong, ZHONG Hua, et al. Optical Bloch oscillation and Zener tunneling in the fractional Schrödinger equation[J]. Scientific Reports, 2017, 7(1): 17872.

[14] CHEN Weijun, WANG Tao, WANG Jie, et al. Dynamics of interacting Airy beams in the fractional Schrödinger equation with a linear potential[J]. Optics Communications, 2021, 496: 127136.

[15] HE Shangling, MALOMED B A, MIHALACHE D, et al. Propagation dynamics of abruptly autofocusing circular Airy Gaussian vortex beams in the fractional Schrödinger equation[J]. Chaos, Solitons & Fractals. 2021, 142: 110470.

[16] SUN Boxuan, CHEN Weijun, LIU Mingshan, et al. Dynamics of Airy beam at interface between linear and nonlinear media[J]. Chinese Journal of Lasers, 2025, 52(10): 1008001.
孙博轩, 陈卫军, 刘名杉, 等. 线性与非线性介质界面处艾里光束的动力学[J]. 中国激光, 2025, 52(10): 1008001.

[17] WANG Qing, ZHANG Lingling, MALOMED B A, et al. Transformation of multipole and vortex solitons in the nonlocal nonlinear fractional Schrödinger equation by means of Lévy-index management[J]. Chaos, Solitons & Fractals, 2022, 157: 111995.

[18] LIU Shilong, ZHANG Yingwen, MALOMED B A, et al. Experimental realisations of the fractional Schrödinger equation in the temporal domain[J]. Nature Communications, 2023, 14(1): 222.

[19] BENDER C M, BOETTCHER S. Real spectra in non-Hermitian Hamiltonians having PT symmetry [J]. Physical Review Letters, 1998, 80(24): 5243.

[20] ABDULLAEV F K, KARTASHOV Y V, KONOTOP V V, et al. Solitons in PT-symmetric nonlinear lattices [J]. Physical Review A, 2011, 83(4): 041805.

[21] LONGHI S. Invisibility in PT-symmetric complex crystals [J]. Journal of Physics A-Mathematical and Theoretical, 2011, 44(48): 485302.

[22] MAKRIS K G, EL-GANAINY R, CHRISTODOULIDES D N, et al. Beam dynamics in PT symmetric optical lattices [J]. Physical Review Letters, 2008, 100(10): 103904.

[23] XIAO Lei, DENG Tianshu, WANG Kunkun, et al. Observation of non-Bloch parity-time symmetry and exceptional points[J]. Physical Review Letters, 2021, 126(23): 230402.

[24] ROY D, AGARWAL G S. Quantum-noise-induced nonreciprocity for single-photon transport in parity-time-symmetric systems[J]. Physical Review A, 2025, 111(1): 013702.

[25] NIXON S, GE Lijuan, YANG Jianke. Stability analysis for solitons in PT-symmetric optical lattices[J]. Physical Review A, 2012, 85(2): 023822.

[26] MUSSLIMANI Z H, MAKRIS K G, EL-GANAINY R, et al. Optical solitons in PT periodic potentials[J]. Physical Review Letters, 2008, 100(3): 030402.

[27] ZHU Xing, WANG Hong, ZHENG Lixian, et al. Gap solitons in parity-time complex periodic optical lattices with the real part of superlattices[J]. Optics Letters, 2011, 36(14): 2680-2682.

[28] HU Sumei, ZHONG Tingting, WU Hongmei, et al. Transmission of multipole solitons in parity-time symmetric scarff potentials[J]. Acta photonica sinica, 2018, 47(9): 0919001.

胡素梅, 钟婷婷, 吴红梅, 等. Parity-Time对称Scarff势中多级孤子的传输特性[J]. 光子学报, 2018, 47(9): 0919001.
[29] WANG Hang, WANG Jiandong. Defect solitons in parity-time periodic potentials[J]. Optics Express, 2011, 19(5): 4030-4035.
[30] KARTASHOV Y V. Vector solitons in parity-time-symmetric lattices[J]. Optics Letters, 2013, 38(14): 2600-2603.
[31] WU Qi, WANG Juanfen, DU Chenrui, et al. Transmission and control of solitons with saturable nonlinear in linear defocusing PT-symmetric waveguide[J]. Acta Photonica Sinica, 2023, 52(6): 0619001.
武琦, 王娟芬, 杜晨锐, 等. 线性散焦PT对称波导中饱和非线性孤子传输与控制[J]. 光子学报, 2023, 52(6): 0619001.
[32] YAO Xiankun, LIU Xueming. Solitons in the fractional Schrödinger equation with parity-time-symmetric lattice potential [J]. Photonics Research, 2018, 6(9): 875-879.
[33] XIE Jiaquan, ZHU Xing, HE Yingji, et al. Vector solitons in nonlinear fractional Schrödinger equations with parity-time-symmetric optical lattices[J]. Nonlinear Dynamics, 2019, 97(2): 1287-1294.
[34] ZHU Xing, YANG Feiwen, CAO Shulei, et al. Multipole gap solitons in fractional Schrödinger equation with parity-time-symmetric optical lattices[J]. Optics Express, 2020, 28(2): 1631-1639.
[35] HUANG Changming, DENG Hanying, ZHANG Weifeng, et al. Fundamental solitons in the nonlinear fractional Schrodinger equation with a PT-symmetric potential[J]. Europhysics Letters, 2018, 122(2): 24002.
[36] ZHONG Ming, YAN Zhenya. Spontaneous symmetry breaking and ghost states in two-dimensional fractional nonlinear media with non-Hermitian potential[J]. Communications Physics, 2023, 6(1): 92.
[37] ZHU Xing, BELIC M R, MIHALACHE D, et al. Two-dimensional gap solitons supported by a parity-time-symmetric optical lattice with saturable nonlinearity and fractional-order diffraction[J]. Optics and Laser Technology, 2025, 184: 112426.
[38] BO Wenbo, WANG Ruru, FANG Yin, et al. Prediction and dynamical evolution of multipole soliton families in fractional Schrodinger equation with the PT-symmetric potential and saturable nonlinearity[J]. Nonlinear Dynamics, 2023, 111(2): 1577-1588.
[39] ZHAI Yuanbo, LI Rujiang, LI Pengfei. Symmetry breaking of partially PT-symmetric solitons in fractional diffraction systems[J]. Acta Optica Sinica, 2024, 44(5): 0519002.
翟远博, 李汝江, 李鹏飞. 分数衍射系统中部分PT对称孤子的对称破缺[J]. 光学学报, 2024, 44(5): 0519002.
[40] WANG Li, ZENG Jianhua, ZHU Yi. Fundamental and dipole gap solitons and their dynamics in the cubic-quintic fractional nonlinear Schrödinger model with a PT-symmetric lattice[J]. Physica D-Nonlinear Phenomena, 2024, 465: 134144.
[41] ZHU Xing, BELIC M R, MIHALACHE D, et al. Two-dimensional gap solitons in cubic-quintic nonlinear media with PT-symmetric lattices and fractional diffraction[J]. European Physical Journal Plus, 2024, 139(12): 1116.
[42] HE Xueqing, ZHAI Yuanbo, CAI Qiang, et al. Symmetry breaking and dynamics of solitons in regular and parity-time-symmetric nonlinear coupler supported by fractional dispersion[J]. Chaos Solitons & Fractals, 2024, 186: 115258.
[43] HU Sumei, MA Xuekai, LU Daquan, et al. Defect solitons in parity-time-symmetric optical lattices with nonlocal nonlinearity[J]. Physical Review A, 2012, 85(4): 043826.
[44] LU Zhien, ZHANG Zhiming. Defect solitons in parity-time symmetric superlattices[J]. Optics Express, 2011, 19(12): 11457-11462.
[45] SZAMEIT A, KARTASHOV Y V, HEINRICH M, et al. Observation of two-dimensional defect surface solitons[J]. Optics Letters, 2009, 34(6): 797-799.
[46] CHEN Wuhe, ZHU Xing, WU T W, et al. Defect solitons in two-dimensional optical lattices[J]. Optics Express, 2010, 18(11): 10956-10962.
[47] HU Sumei, HU Wei. Defect solitons in saturable nonlinearity media with parity-time symmetric optical lattices[J]. Physica B: Condensed Matter, 2013, 429: 28-32.
[48] XIE Jianing, SU Zhikun, CHEN Weicheng, et al. Defect solitons in two-dimensional photonic lattices with parity-time symmetry[J]. Optics Communications, 2014, 313: 139-145.
[49] HU Sumei, HU Wei. Defect solitons in optical lattices with parity-time symmetric defect[J]. The European Physical Journal D, 2012, 66(10): 266.
[50] HUANG Changming, DONG Liangwei. Gap solitons in the nonlinear fractional Schrodinger equation with an optical lattice [J]. Optics Letters, 2016, 41(24): 5636-5639.
[51] DONG Liangwei, HUANG Changming, QI Wei. Nonlocal solitons in fractional dimensions[J]. Optics Letters, 2019, 44(20): 4917-4920.
[52] WANG Shengyao, XIA Tuanjie, CHEN Weijun, et al. Defect solitons supported by optical lattice with saturable nonlinearity in fractional Schrödinger equation[J]. Physica Scripta, 2023, 98(7): 075207.
[53] WANG Shengyao, CHEN Weijun, LIU Wenjie, et al. Two-dimensional line defect lattice solitons in nonlinear fractional

Schrödinger equation[J]. Optics & Laser Technology, 2024, 175: 110870.
[54] YANG Jianke. Nonlinear waves in integrable and nonintegrable systems[M]. Philadelphia: Society for Industrial and Applied Mathematics, 2010: 90-98.

Defect Solitons in PT-symmetric Optical Lattices with Fractional Diffraction

XIA Tian, CHEN Weijun, SUN Boxuan, WANG Jingyu, WU Chuyao, XIA Haoran, ZHAO Peng, WANG Liankai, SONG De
(*School of Physics, Changchun University of Science and Technology, Changchun* 130022, *China*)

Abstract: Optical lattice solitons, as key entities at the intersection of nonlinear optics and photonics, not only provide an ideal model for uncovering fundamental physical principles of nonlinearity and periodicity coupling, but also break through technical bottlenecks in conventional optical transmission, manipulation, and storage. A considerable number of studies have been reported on the existence and stability of defect solitons under both normal and fractional diffraction mechanisms. However, the properties of defect solitons in optical lattices under the combined influence of fractional effects and PT-symmetric potentials have not been thoroughly investigated. This paper focuses on studying the existence, stability, and propagation dynamics of defect solitons in PT-symmetric optical lattices with fractional diffraction, examining the impact of fractional effects and defect types on the bandgap structure, analyzing the existence domain of defect solitons, elucidating their linear stability, and discussing the influence of system parameters on the characteristics of defect solitons.

A theoretical model for optical wave propagation in Kerr nonlinear optical lattices with PT-symmetric potentials under fractional-order effects is established based on the fractional nonlinear Schrödinger equation. The plane wave expansion method is used to analyze the effects of defect strength and fractional-order characteristics on the bandgaps of defect solitons. The modified squared-operator iteration method is employed to numerically solve the model and obtain steady-state solutions of the defect solitons. Additionally, perturbations are introduced to the steady-state solutions, and linear stability analysis is performed using the Fourier collocation method. Finally, the propagation properties of the solitons are verified by means of the symmetrized split-step Fourier method.

The bandgap range of the optical lattice narrows as the Lévy index decreases. As the defect strength increases from negative to positive, the semi-infinite gap gradually narrows, while the other bandgaps progressively widen. Under negative defect conditions, the power of solitons in both the semi-infinite gap and the first gap generally decreases with increasing propagation constant, except for an initial increase followed by a decrease in the low-power region of the semi-infinite gap and the medium-power region of the first gap. As the Lévy index varies, the stable region of solitons in the semi-infinite gap gradually shrinks, while solitons in the first gap remain unstable. Under zero defect conditions, the soliton power in both the semi-infinite and first gaps decreases monotonically with the propagation constant. The influence of the Lévy index on soliton stability is similar to that under negative defects. Under positive defect conditions, the soliton power in both gaps decreases with increasing propagation constant, but a cutoff point exists where the power reaches zero. Moreover, a smaller α results in a smaller propagation constant at the cutoff point. Similarly, a decrease in α reduces the stable region of solitons in the semi-infinite gap, although stable solitons exist in the first gap. Additionally, for all three defect types, the width of the defect soliton envelope narrows slowly as α decreases, while the peak intensity increases gradually. The power decreases with reduced α, and the peak intensity of the soliton envelope decreases as the defect strength changes from negative to positive.

This study investigates the existence, stability, and propagation dynamics of defect solitons in PT-symmetric optical lattices with fractional diffraction. Under fractional diffraction, as the Lévy index increases, the power of defect solitons in the semi-infinite bandgap and the first bandgap gradually increases for all defect lattices, while the stability of solitons improves. In cases of negative defects and zero

defects, defect solitons only have stable intervals in the semi-infinite bandgap and are completely unstable in the first bandgap. In cases of positive defects, defect solitons have stable intervals in both the semi-infinite bandgap and the first bandgap. Additionally, within the semi-infinite bandgap, as the Lévy index decreases, the peak of the defect soliton envelope increases while its width narrows; as the propagation constant increases, the peak of the defect soliton envelope decreases rapidly. Within the first bandgap, the peak of the soliton envelope decreases as the Lévy index decreases and decreases as the propagation constant increases under positive defect conditions. In summary, the envelope, power, and stability of defect solitons are significantly influenced by the defect strength, Lévy index, and propagation constant.

Key words: Nonlinear optics; Parity-time-symmetric; Defect solitons; Fractional diffraction; Kerr effect

OCIS Codes: 190.0190; 190.6135; 000.4430

CSTR: 32255.14.gzxb20265502.0219003

Foundation item: Natural Science Foundation of Jilin Province (YDZJ202301ZYTS377), National Natural Science Foundation of China (U2141239, 12274041), Construction of Independent Innovation Capability for the Jilin Provincial Engineering Research Center of Optoelectronic Detection and Multidimensional Information Processing (2021C032)